Plasma chemistry in fluorocarbon film deposition from pentafluoroethane/argon mixtures

Sairam Agraharam, Dennis W. Hess,[a] Paul A. Kohl, and Sue A. Bidstrup Allen
School of Chemical Engineering, Georgia Institute of Technology, Atlanta, Georgia 30332

(Received 2 April 1999; accepted 16 July 1999)

Plasma-enhanced deposition of fluorocarbon films was performed at 120 °C from a mixture of pentafluoroethane (CF_3CHF_2) and argon in a parallel plate plasma reactor. Mass spectrometry of the reactor effluent was used to gain an understanding of the plasma chemistry of this monomer. The monomer primarily dissociated into $CF_3^{\bullet}$ and $CHF_2^{\bullet}$ in the plasma. The results from mass spectrometry indicated that CHF_2^{*} was the primary precursor for deposition and that the fluorine radicals in the plasma were primarily scavenged as CF_4 and HF. Monomer conversion (fraction of monomer fragmented) in the plasma was determined based on mass spectrometer partial pressure analysis of CH_3CHF^+ fragments (parent molecule: CF_3CHF_2) before and after plasma ignition. The conversion correlated directly with both the applied power and the deposition rate. The overall gas phase reactions did not change significantly with rf power within our range of operation, indicating a common reaction mechanism at all powers. No significant change in the composition of the deposited films was found, as measured by x-ray photoelectron spectroscopy (XPS), supporting the common mechanism conclusion. Further, XPS studies showed a fluorine-to-carbon ratio between 1.05 and 1.15 suggesting extensive crosslinking of the polymer. Infrared spectra of the deposited films showed negligible CH_x concentration despite the presence of hydrogen in the monomer.
 [S0734-2101(99)01906-5]

I. INTRODUCTION

The tremendous enhancement in the performance and operating speed of microprocessors has been driven primarily by the continuous reduction of device dimensions and consequently, an increase in the packing density of transistors in integrated circuits (ICs). However, as device sizes shrink below 0.25 μm, the signal transmission delay or the *RC* delay (*R*—resistance of the interconnect, *C*—capacitance of the dielectric) becomes the limiting factor in determining IC speed. Since both transmission delay and power consumption critically depend on the dielectric constant of the insulator between the interconnects, it is necessary to develop new interlevel dielectrics with dielectric constants (k) significantly lower than conventional silicon dioxide ($k = 3.9-4.2$).[1,2] Many different low-k materials have been investigated including fluorinated silicon oxides,[3] inorganic and organic materials,[4,5] and porous materials such as xerogels,[6] and aerogels.[7] Plasma deposited fluoropolymers[8,9] are promising candidates since they have low dielectric constants, ranging from 1.8 to 2.5, high thermal stability, chemical inertness, and low moisture absorption. Fluoropolymers have been deposited from mixtures of C_4F_8 and C_2H_2 with dielectric constants less than 2.4 and thermal stability greater than 400 °C.[9] However, environmental concerns regarding the long atmospheric lifetimes of fluorocarbon monomers have prompted the search for alternative precursors. One promising solution is the use of hydrofluorocarbons (e.g., CHF_3, CF_3CHF_2), that have relatively shorter atmospheric lifetimes and do not produce environmentally detrimental degradation products.[10]

Previous work[11] on the plasma deposition of films from CHF_3 indicated that the deposition rate with CHF_3 was much higher than with pure fluorocarbons like CF_4, C_2F_6, and C_3F_8. This was attributed to the higher precursor concentration and the lower free fluorine generation[12] in CHF_3 plasmas relative to the plasmas of fluorocarbons. X-ray photoelectron spectroscopy (XPS) analyses showed that films deposited from CHF_3 were more highly crosslinked than those from C_3F_8, and thus were expected to have higher thermal stability. Recently, dielectric constants of 2.4 have been reported for fluorocarbon films grown by pulsed plasma deposition of $C_2H_2F_4$ and CH_2F_2.[13] The fluorine to carbon ratio for films deposited from $C_2H_2F_4$ and CH_2F_2 was 0.91 and 0.64, respectively. XPS analyses showed that the dominant bonding configurations in the films were $C-CF_x$ and that the CF_3 content was lowest for the precursor having the lowest F:H ratio. The dominance of $C-CF_x$ structures was attributed to HF elimination reactions. However, this conclusion was based on the structure of the resultant films, and no experiments were performed to monitor the gas phase chemistry. Thus, it is useful to investigate other hydrofluorocarbons with a view to studying as well as improving the properties of deposited fluorocarbon films. Furthermore, very little work has been reported that seeks to understand the plasma chemistry of these hydrofluorocarbons.

Pentafluoroethane (CF_3CHF_2), with argon as the carrier gas, was the monomer used in the current study. To our knowledge, this is the first plasma deposition study that has been reported on this monomer. Mass spectrometry, x-ray photoelectron spectroscopy and infrared spectroscopy were used to gain insight into the monomer plasma chemistry and chemical bonding information of the deposited films.

[a]Electronic mail: dennis.hess@che.gatech.edu

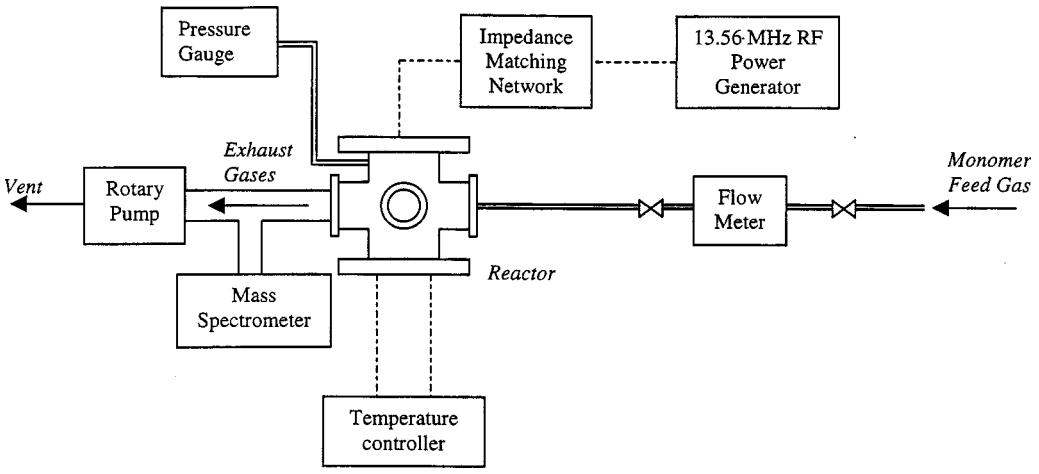

FIG. 1. Schematic of the parallel plate plasma reactor system used for fluoropolymer film deposition.

II. EXPERIMENTAL DETAILS

A parallel plate radio frequency (rf) plasma reactor was used to deposit fluorocarbon polymer films. A schematic of the reactor design is shown in Fig. 1. The reactor was a stainless-steel six-way cross, capped by ultrahigh vacuum flanges at the top and bottom. Electrodes were 4 cm diameter circular stainless steel disks, which were electrically isolated from other parts of the reactor. The distance between the electrodes was fixed at 2.9 cm for all experiments. RF power at 13.56 MHz was generated using an ENI Power Systems HF-300 rf generator and was coupled to the top electrode through a Heathkit SA-2060A antenna tuner. The lower electrode was electrically grounded and heated with Omegalux CIR 2015 cartridge heaters. The temperature was controlled using a Syskon RKC temperature controller. Substrates were placed on the grounded electrode, which was maintained at a constant temperature of 120 °C. The monomer pentafluoroethane (Dupont HFC 125) was mixed with argon (Air products, 99.99% purity) and their flowrates regulated by teflon flowmeters. The flowrates of argon and pentafluoroethane were constant at 75 and 20 sccm, respectively, for all depositions. Chamber pressure was monitored with a Kurt J. Lesker wide range vacuum gauge capable of measuring from 1500 Torr to 1 mTorr. The base pressure in the chamber was less than 9 mTorr, while the operating pressure was 1 Torr for all depositions. The reactor was evacuated with an Alcatel 2063 C rotary vacuum pump through one side port, while reactants were introduced from the opposite side.

The composition of the exhaust gases from the reactor was monitored with a quadrupole mass spectrometer that measured species with mass-to-charge ratios between 1 and 300 amu. The ionizer potential in the mass spectrometer was set at 70 eV. The sampling orifice of the mass spectrometer was approximately 30 cm downstream from the active plasma region. Therefore, the mass spectrometer sampled the recombination products of the free radicals from the plasma. The orifice diameter was adjusted so that the total pressure in the mass spectrometer was always below 10^{-5} Torr and was constant for all runs at the same pressure. Mass spectra were taken before and at 5 and 8 min after plasma ignition. The partial pressure of specific species was monitored with time in order to evaluate the effect of the plasma. Further, the concentration of common background species like water, nitrogen and carbon dioxide were monitored. Their partial pressures were constant throughout the deposition.

Infrared spectroscopy was used to evaluate the chemical structure of the deposited films using a Nicolet Magna-IR 560 Fourier transform infrared (FTIR) spectrometer equipped with a deuterated triglicine sulphate (DTGS) detector. Infrared spectra were collected in reflection mode at a grazing angle of 70°. All spectra were taken at a resolution of 4 cm^{-1} and averaged over 512 scans. The polymers were deposited on titanium for infrared analysis. Polymer thicknesses, measured using a Dektak profilometer, were between 1.5 and 2 μm.

XPS was used to determine the relative composition and chemical bonding structure of the films. In order to alleviate the effects of differential charging, very thin films ranging from 5 to 10 nm deposited on titanium were used for analysis. Spectra were collected using a PHI model 1600 spectrometer. X rays were generated using a water-cooled Al $K\alpha$ anode operated at a power of 350 W and monochromatized by a quartz crystal. The monochromatic x rays impinged on the sample at an angle of 45° from the detector axis. A 180° hemispherical analyzer and a multichannel detector provided high sensitivity and high energy resolution. Chamber pressure was typically below 5×10^{-9} Torr during analysis. An electron pass energy of 11.75 eV was used to analyze the regions of interest in each sample. The C 1*s*, F 1*s*, O 1*s*, N 1*s*, and Ti 2*p* photoelectrons were analyzed. The binding energy shifts were corrected for surface charging by aligning the highest binding energy C 1*s* peak to 293.2 eV. Finally, curve fitting was performed on each spectral region assuming all peaks to be perfectly Gaussian and to have the same full width half maximum (FWHM).

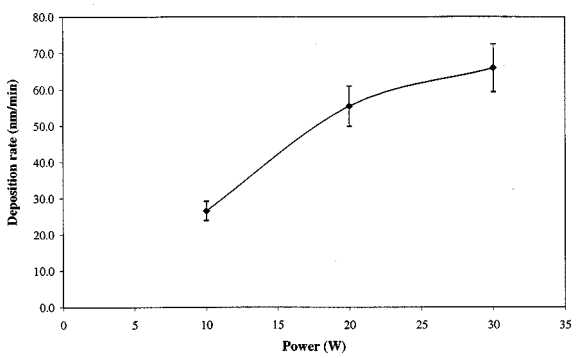

FIG. 2. Deposition rate (nm/min) as a function of applied power (W) at a total pressure of 1 Torr and 120 °C substrate temperature.

III. RESULTS

The effect of applied power on the polymer deposition rate is shown in Fig. 2. The deposited film thickness was typically between 1 and 2 μm, depending on the applied power and the deposition time. At a pressure of 1 Torr, the deposition rate increased from 26.5 to 65.9 nm/min as the applied power increased from 10 to 30 W. This indicates that the deposition process was carried out in the power-limited regime and further increases in the deposition rate may be expected by increasing the power.

XPS analyses were carried out on the deposited films. Initial survey spectra indicated the presence of fluorine, carbon and a very small amount of oxygen in the films. High-resolution spectral analyses of C 1*s*, F 1*s*, and O 1*s* indicate a F/C ratio between 1.05 and 1.15 and an O/C ratio less than 0.04 for all films. The low F/C ratio indicates that the deposited films are highly crosslinked. This extensive crosslinking is consistent with previous observations[9] for films deposited from CHF_3. Since the oxygen content of the films is so low, peak deconvolution of the C 1*s* spectra is carried out assuming carbon to be bonded to only fluorine or CF_x species. The C 1*s* spectrum is deconvoluted into five Gaussian peaks corresponding to $\underline{C}F_3$ (293.2 eV), $\underline{C}F_2$ (290.95 eV), $\underline{C}F$ (288.8 eV), $\underline{C}-CF_x$ (286.5 eV), and $\underline{C}-\underline{C}$ or $\underline{C}-H$ (284.9 eV) with a constant FWHM of 1.5 eV. The order of these peaks in terms of decreasing binding energy matches that obtained by other authors.[9,11,14–17] Further, the absolute binding energies of CF_3,CF_2,CF,C–CF_x and C–C fall within the range of published literature values[9,11,14–17,26] from 292.6 to 295, 290.3 to 293, 288 to 290, 285.5 to 287.3, and 283.4 to 286 eV, respectively. The C–CF_x peak at 286.5 eV is due to electrons originating from the secondary carbon bonded to CF_x groups while the C–C or C–H peak at 284.9 eV corresponds to carbon that is neither bonded to fluorine nor to any CF_x groups. A typical C 1*s* spectrum of the deposited film is shown in Fig. 3. The C–C or C–H peak at 284.9 eV accounts for only 2–4% of the total C 1*s* area and is partially due to adventitious carbon found on all sample surfaces. The composition variation of the film with rf power is shown in Fig. 4; essentially no variation is observed. In all cases, the largest peak corresponds to the C–CF_x consistent with our expectation of a highly crosslinked film. This agrees with

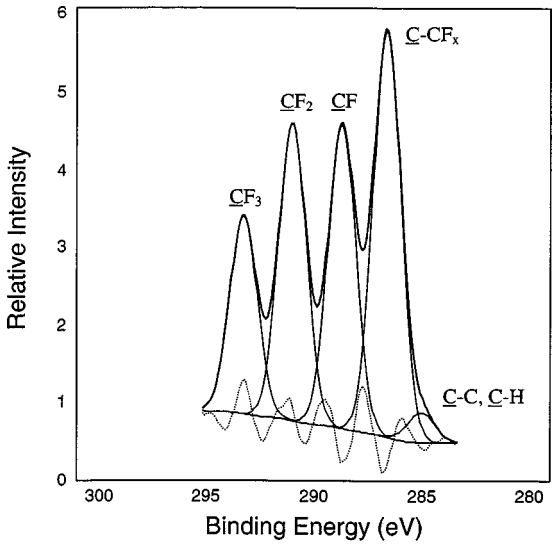

FIG. 3. High-resolution C 1*s* spectrum of a polymer film obtained by XPS analysis at a pass energy of 11.75 eV. Deposition conditions: 30 W, 120 °C, 1 Torr.

previous results[13] obtained from pulsed plasma deposition of CH_2F_2 and $C_2H_2F_4$. However, the F/C ratio and % CF_3 of our films are higher than those in Ref. 13 despite the fact that depositions were carried out in a continuous wave plasma at a much higher substrate temperature. The higher F/C ratio and the % CF_3 observed in the present study appear to be due to higher F/H and F/C ratios in C_2HF_5 relative to CH_2F_2 and $C_2H_2F_4$.

A typical infrared spectrum of a polymer film is shown in Fig. 5. The infrared spectrum shows a broad absorption peak between 980 and 1450 cm^{-1}; this is a common characteristic of plasma-deposited fluorocarbon films that indicates the presence of a variety of CF_x species randomly distributed throughout the film, and is attributed to all CF_x ($x=1,2,3$) stretching modes.[13,18] The other major broad peak between 1600 and 1850 cm^{-1} is due to a variety of unsaturated fluorocarbon bonds[19] and nonconjugated alkenes[20] such as

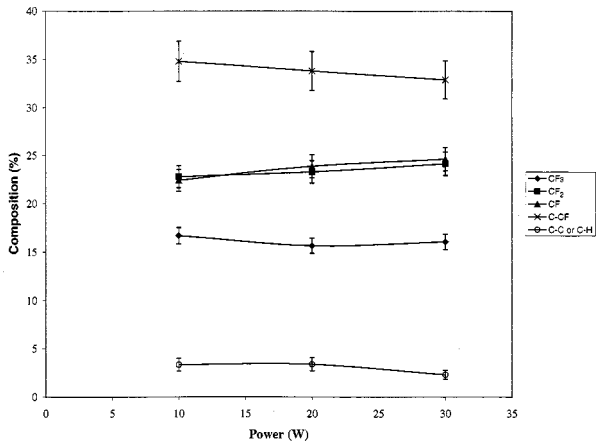

FIG. 4. XPS composition (%) of CF_3, CF_2, CF, C–CF_x, and C–C or C–H in a deposited polymer film as a function of applied power (W). Substrate temperature: 120 °C, total pressure: 1 Torr.

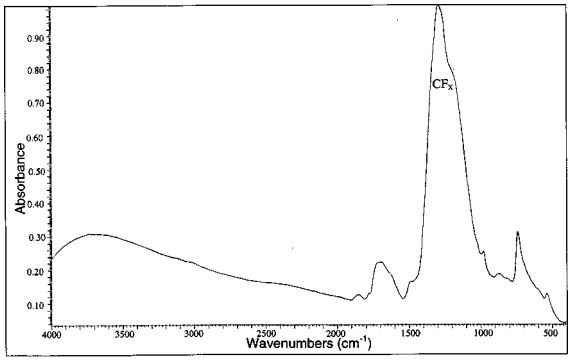

FIG. 5. Infrared spectrum of a deposited polymer film. Deposition conditions: 20 W, 120 °C, 1 Torr, 1 h.

TABLE I. Relative concentrations of major mass spectrometer fragments of the pure monomer normalized to the CHF_2^+ fragment.

Atomic mass	Fragment	Relative concentration
51	CHF_2^+	100
101	CF_3CHF^+	21.9
69	CF_3^+	24
119	$C_2F_5^+$	0.9
20	HF^+	1.2
50	CF_2^+	14.9
81	$C_2F_3^+$	3.4
31	CF^+	14.5
32	CHF^+	23.7
100	$C_2F_4^+$	5.3

$-C=CF_2$, $-CF=CF_2$, $-C\equiv C$ or to oxygenated species like $-C=O$ and $-CF\equiv O$ (1833 cm^{-1})[21] which may originate from residual oxygen present in the reactor during deposition or, most likely, from post-deposition oxidation. However, the low O/C ratio from XPS analysis indicates that this peak is most likely due to unsaturated fluorocarbon bonds. The peak at 740 cm^{-1} could be interpreted as either an amorphous teflon (PTFE) stretch[22] or a CF_2 symmetric stretch, and has been shown to reflect crosslinking of the film.[23] Indeed, the 740 cm^{-1} peak is observed in the infrared spectrum of pure PTFE.[24] An important feature of the infrared spectra is the negligible intensity of sp^2 and sp^3 CH_x peaks between 2800 and 3000 cm^{-1} in all samples despite the presence of hydrogen in the monomer. The intensity of the CH_x peaks is at least two orders of magnitude lower than that of the major fluorocarbon peak. Similarly, low hydrogen content has been observed in films deposited from C_2F_6/H_2 mixtures in an inductively coupled plasma reactor when the C_2F_6 content in the feed was 70% or greater by mass.[14] Also, low hydrogen content was reported in films obtained from pulsed plasma deposition of $C_2H_2F_4$ and CH_2F_2 monomers.[13] Hence, it may be possible to deposit nearly pure fluorocarbon films with little hydrogen and all the requisite properties, such as low dielectric constant, low refractive index and high thermal stability, from hydrofluorocarbon monomers at elevated temperatures.

Mass spectrometric analyses have been performed on the effluent from the reactor in order to gain insight into the plasma chemistry. To our knowledge, this is the first attempt to characterize the plasma gas phase chemistry of this monomer using mass spectrometry. Only positive ions created by the ionization in the mass spectrometer are analyzed. Table I shows the major mass fragments of the pure monomer (without argon) fed directly to the mass spectrometer (no plasma) and their relative concentrations with respect to CHF_2^+ (assigned a value of 100). This peak has also been observed in a mass spectrometer study of a CHF_3 plasma.[25] The high concentration of CHF_2^+ demonstrates a high probability for C–C bond cleavage in the monomer. All experiments using plasma excitation were carried out with both argon and monomer in the feed.

When the plasma is ignited, the species detected in the mass spectrometer that undergo significant changes in concentrations are CHF_2^+, CF_3CHF^+, CF_3^+, and HF^+. Figure 6 shows the variations of these species relative to their initial concentrations (without the plasma) as the applied power is increased. Clearly, the concentrations of CHF_2^+ and CF_3CHF^+ decrease with applied power, while the concentrations of CH_3^+ and HF^+ increase. Further, there is a small increase in the concentrations of $H^+(1)$, $H_2^+(2)$, $C_2F_5^+(119)$, $C_2F_3^+(81)$, $C_2F_3H^+(82)$, $C_2F_3H_2^+(83)$, $C_2F_3H_3^+(84)$, $C_3F_3^+(93)$, $C_3F_3H^+(94)$, $C_3F_3H_2^+(95)$, $C_3F_3H_3^+(96)$, and $C_3F_3H_3^+(97)$ for all applied powers when the plasma is ignited. In addition, there is a minor decrease in CF^+ and CHF^+ concentrations due to the plasma. At all applied powers, the observed peak with the highest mass-to-charge ratio was 131, which corresponds to $C_3F_5^+$.

IV. DISCUSSION

Based on the mass spectrometer data, electron impact dissociation of the monomer appears to occur at the C–C bond rather than the C–H bond. This can be seen from the low concentration of $C_2F_5^+$ in the mass spectrum of the pure monomer (Table I). Such observations are consistent with the bond energies[20] and bond lengths[27] of the C–C, C–F, and C–H bonds shown in Table II. It should be noted however, that the bond energies of C–F and C–C displayed in Table II

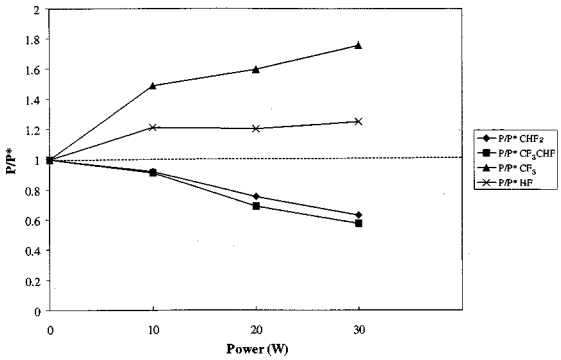

FIG. 6. Plot of P/P^* vs applied power (W). P^* and P refer to the partial pressure of a particular mass spectrometer fragment before and 5 min after plasma ignition, respectively. Substrate temperature: 120 °C, operating pressure: 1 Torr.

TABLE II. Bond energies and bond lengths of C–H, C–F, and C–C bonds.

Bond	Distance (nm)	Energy (kJ/mole)
C–H	0.109	431
C–F	0.1335	523
C–C	0.1525	406

are based on CF_4 and C_2F_6, respectively. Clearly, the exact binary bond energies are dependent on the parent molecule; Table II displays the bond energy trends.

The C–C bond is the weakest of the three bonds shown in Table II and has the longest atom-to-atom distance, thus providing a higher cross-section for undergoing electron impact collisions. Further, it is plausible that although the C–F bond is stronger than the C–H bond, some fraction of C–F bonds will be broken because of their relatively high cross section for dissociation. This is shown by the fact that the CF_3CHF^+ concentration is much higher than that of $C_2F_5^+$ in the mass spectrum of the pure monomer. Thus, when the plasma is ignited, monomer dissociation is very likely to occur at the C–C bond due to gas phase collisions with electrons and with argon metastable species (Ar*). We believe that the primary dissociation mechanisms for the monomer in the plasma are:

$$CF_3CHF_2 + e^- \text{ or } Ar^* \rightarrow CF_3^{\bullet} + CHF_2^{\bullet}, \quad (1)$$

$$CF_3CHF_2 + e^- \text{ or } Ar^* \rightarrow CF_3CHF^{\bullet} + F^{\bullet}. \quad (2)$$

The other trend clearly observed in Fig. 6 is the increase of CF_3^+ partial pressure detected by the mass spectrometer when the plasma is ignited. The increase in CF_3^+ partial pressure is likely due to plasma-induced fragmentation of $CF_3CHF^{\bullet}$.

$$CF_3CHF^{\bullet} + e^- \text{ or } Ar^* \rightarrow CF_3^{\bullet} + CHF^{\bullet}. \quad (3)$$

Furthermore, the increase in CF_3 indicates that a major portion of the $CF_3^{\bullet}$ produced by fragmentation of the monomer does not participate in the deposition, but rather forms stable gas phase species, most likely CF_4 (mass spectrometer fragment: CF_3^+), although CHF_3 may also form by reaction of $CHF_2^{\bullet}$ and $F^{\bullet}$.

$$CF_3^{\bullet} + F^{\bullet} \rightarrow CF_4. \quad (4)$$

In addition, the increase in $C_2F_5^+$ concentration with plasma ignition indicates the gas phase recombination of $CF_3^{\bullet}$ either with another $CF_3^{\bullet}$ or via a two-step process involving the sequential addition of $CF_2^{\bullet}$ and $F^{\bullet}$ to form C_2F_6. Although the F/C ratio of the monomer is 2.5, the deposited polymer has a F/C ratio of only 1.1, thus necessitating an increase in gas phase F-rich species. Hence, the increase in gas phase F-rich species such as CF_4 and C_2F_6 accounts for the conservation of fluorine species in the system.

Although recombination of $CF_3^{\bullet}$ or reaction with $F^{\bullet}$ is very likely, XPS analyses show the presence of CF_3 in the deposited films and thus a small fraction of the $CF_3^{\bullet}$ is directly incorporated into the film. Also, some $CF_3^{\bullet}$ is converted to $CF_2^{\bullet}$ through gas phase collisions as shown in reaction (5) which requires electron energies of only 2.2 eV;[17] electrons of this energy are abundant in the plasma.

$$CF_3^{\bullet} + e^- \rightarrow CF_2^{\bullet} + F^{\bullet} + e^-. \quad (5)$$

Further fragmentation of $CF_2^{\bullet}$ to $CF^{\bullet}$ requires a high electron threshold energy of 6.1 eV[17] and hence is not particularly favorable. In addition, the rate coefficient for recombination of $CF_2^{\bullet}$ with $F^{\bullet}$ is nearly two orders of magnitude lower than that for the reaction of $CF_3^{\bullet}$ with $F^{\bullet}$.[28] Therefore, the relatively stable $CF_2^{\bullet}$ radical is consumed in the plasma primarily either by incorporation into the growing film or by reaction with $CF_2^{\bullet}$ and $CHF^{\bullet}$ species, rather than by reaction with $F^{\bullet}$ radicals in the plasma. The high concentration of CF_2 in the deposited film (as determined by XPS analysis) supports the contribution of $CF_2^{\bullet}$ to film formation while the recombination mechanism is confirmed by the increase in $C_2F_3^+(C_2F_4)$ and $C_2F_3H^+(C_2F_3H)$concentrations in the mass spectrometer when the plasma is ignited.

The increase in the concentration of HF^+ (parent molecule: HF) with the ignition of the plasma may be due to hydrogen scavenging of free fluorine radicals in the gas phase or to surface reactions occurring on the growing polymer surface. However, the primary reaction accounting for the formation of HF can not be ascertained from the current study. The negligible accounts of F^+ and F_2^+ in the effluent gas indicate that most of the free fluorine is removed from the system as CF_4 [reaction (4)] and HF.

The decrease in the concentrations of CF_3CHF^+ (parent molecule: CF_3CHF_2) and CHF_2^+ in Fig. 6 is consistent with the consumption of the monomer, either by polymer formation or by reaction with other gas phase species. The fraction of the monomer fragmented in the reactor can be determined by partial pressure analysis of CF_3CHF with and without the plasma and is referred to as conversion (X). Conversion is defined by

$$X = 1 - \frac{P_{CF_3CHF}}{P_{CF_3^*CHF}}. \quad (6)$$

The variation of monomer conversion with applied power is shown in Fig. 7. Conversion increases with applied power, as expected, and correlates with the observed deposition rates, as shown in Fig. 8. The conversion at the highest power, 30 W, is only 0.42, indicating an excess of monomer in the reaction mixture. Based on the XPS concentrations in Fig. 4, there appears to be no significant change in the F/C ratio or the concentrations of the various species in the deposited films with applied power. The same trend is observed in the mass spectral analysis of the reactor effluent at all rf powers. Also, there are no additional peaks or significant changes in the relative concentrations of the effluent species with increases in rf power. Finally, no peaks with higher mass-to-charge ratio than $C_3F_5^+$ (131) are observed in any deposition experiment within the 1 to 300 amu range of the mass spectrometer. Thus, the overall reaction mechanism appears to be the same at all applied power levels. Further, there is an increase in the gas phase CF_3^+ (fluorine rich) concentration with the monomer conversion as observed

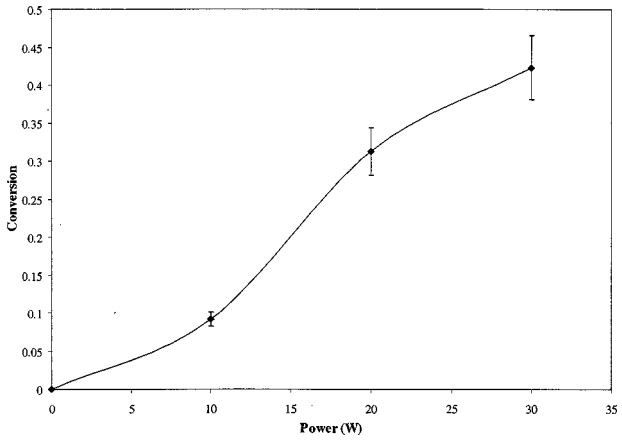

FIG. 7. Monomer conversion as a function of applied power (W). Note that, conversion refers to the fraction of the monomer fragmented in the plasma. Substrate temperature: 120 °C, operating pressure: 1 Torr.

from Fig. 6 and Fig. 8. This increase in F-rich species can be attributed to the fluorine conservation requirement in the reaction system. Since the F/C ratio of the deposited films is only 1.1 and is independent of monomer conversion and polymer deposition rate, the concentration of gas phase F-rich species must increase with monomer conversion in order to balance the high F/C ratio (2.5) of the monomer.

Further insight into the plasma chemistry can be obtained by noting that the primary plasma dissociation products of the monomer are $CF_3^{\bullet}$ and $CHF_2^{\bullet}$ [reaction (1)]. Therefore, a large decrease in the mass spectrometer concentrations of CHF_2^+ coupled with an increase in CF_3^+ (Fig. 6) on plasma ignition indicates that $CHF_2^{\bullet}$ may be the primary precursor for deposition, although it may undergo further fragmentation in the gas phase.

The increase in the concentration of H_2^+, HF^+, $C_2F_3H^+(82)$, $C_2F_3H_2^+(83)$, $C_2F_3H_3^+(84)$, $C_3F_3H^+(94)$, $C_3F_3H_2^+(95)$, $C_3F_3H_3^+(96)$, and $C_3F_3H_4^+(97)$ species demonstrates radical recombination and accounts for the removal of hydrogen from the plasma and from the deposited film. The F/C ratio of 1.1 in the deposited films can be explained by assuming that $CHF_2^{\bullet}$ is the primary film precursor and that argon bombardment of the growing films modifies the film composition and structure. However, the exact processes and reactions leading to the removal of hydrogen, and the method by which argon bombardment crosslinks the film (reduced F/C ratio) cannot be explained simply by the gas phase chemistry. Rather, this fact depends strongly on the surface chemical reactions and ion-surface interactions. Bombardment by ions and argon metastable species helps to remove loosely bound fragments such as H, F, CF, and CH and produces adsorption sites for polymerizing precursors. Also, polymer crosslinking can be enhanced by fluorine scavenging from the deposited film by hydrogen radicals; likewise, film H can be scavenged by F atoms. Similarly, previous investigations have suggested HF scavenging by the interaction of adjacent CH_x and CF_x bonds on the polymer surface.[11] Such HF scavenging mechanisms could account for the high $C-CF_x$ concentration and the low hydrogen content of the deposited films in the present study.

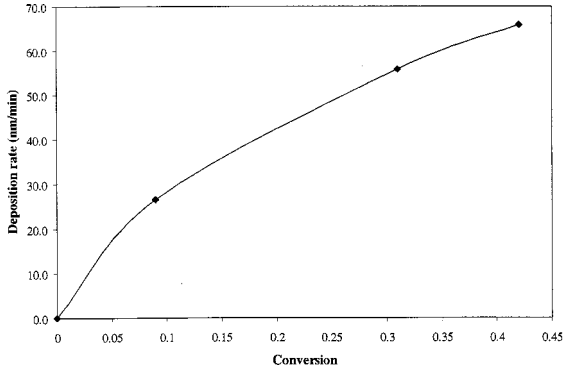

FIG. 8. Polymer deposition rate (nm/min) as a function of monomer conversion. Substrate temperature: 120 °C, operating pressure: 1 Torr.

V. CONCLUSIONS

We have shown that at 1 Torr in a 75 sccm Ar/20 sccm pentafluoroethane rf plasma, pentafluoroethane dissociates primarily into $CF_3^{\bullet}$ and $CHF_2^{\bullet}$ moieties in the plasma. Mass spectrometry studies suggest that $CHF_2^{\bullet}$ is the primary film deposition precursor while only a small fraction of $CF_3^{\bullet}$ aids in the deposition. A majority of the free fluorine radicals in the system are scavenged as HF and CF_4. Conversion of the monomer can be determined from CF_3CHF^+ fragment partial pressure measurements; the deposition rate directly correlates with this conversion. Since no new or additional species are detected by mass spectrometry, it appears that the reaction mechanism does not vary with rf power within our range of operation. This conclusion is consistent with the insignificant changes in the composition (as determined by XPS) of the deposited films with changes in rf power. The F/C ratio of ~1.1 for the deposited films indicates that the films are highly crosslinked. The crosslinking can be attributed to the effect of argon bombardment as well as to fluorine scavenging from the film by hydrogen radicals. Further, infrared analyses of the deposited films indicate that the films contain very little if any, hydrogen. Hence, nearly hydrogen free fluoropolymer layers can be formed at 120 °C substrate temperature from a mixture of argon and pentafluoroethane despite the presence of hydrogen in the monomer structure.

ACKNOWLEDGMENTS

The authors wish to thank Dr. Mike Mocella (Dupont) for supplying the pentafluoroethane monomer used in this study, and Shilpa Thanawalla for the initial design of the reactor setup.

[1]R. K. Laxman, Semicond. Int. **5**, 71 (1995).
[2]P. Singer, Semicond. Int. **5**, 88 (1996).
[3]K. Kim, D. Kwon, and G. S. Lee, Thin Solid Films **332**, 369 (1998).
[4]N. H. Hendricks, K. S. Yau, A. R. Smith, and W. B. Wan, Mater. Res. Soc. Symp. Proc. **381**, 59 (1995).
[5]Y. K. Lee, S. P. Murarka, S. P. Jeng, and B. Auman, Mater. Res. Soc. Symp. Proc. **381**, 31 (1995).
[6]D. M. Smith, J. Anderson, C. C. Gho, G. P. Johnson, and S. P. Jeng, Mater. Res. Soc. Symp. Proc. **381**, 261 (1995).

[7]L. W. Hrubesh, Mater. Res. Soc. Symp. Proc. **381**, 267 (1995).
[8]K. Endo and T. Tatsumi, Mater. Res. Soc. Symp. Proc. **381**, 249 (1995).
[9]S. Takeishi, H. Kudo, R. Shinohara, M. Hoshino, S. Fukuyama, J. Yamaguchi, and M. Yamada, J. Electrochem. Soc. **144**, 1797 (1997).
[10]J. S. Francisco and M. M. Maricq, Acc. Chem. Res. **29**, 391 (1996).
[11]P. J. Astell-Burt, J. A. Cairns, A. K. Cheetham, and R. M. Hazel, Plasma Chem. Plasma Process. **6**, 417 (1986).
[12]A. J. Bariya, H. Shan, C. W. Frank, S. A. Self, and J. P. McVittie, J. Vac. Sci. Technol. B **9**, 1 (1991).
[13]C. B. Labelle, K. K. S. Lau, and K. K. Gleason, Mater. Res. Soc. Symp. Proc. **511**, 75 (1998).
[14]N. M. Mackie, N. F. Dalleska, D. G. Castner, and E. R. Fisher, Chem. Mater. **9**, 349 (1997).
[15]H. Yasuda and C. R. Wang, J. Polym. Sci., Part A: Polym. Chem. **23**, 87 (1985).
[16]M. J. O'Keefe and J. M. Rigsbee, Mater. Res. Soc. Symp. Proc. **304**, 179 (1993).
[17]A. M. Hynes, M. J. Shenton, and J. P. S. Badyal, Macromolecules **29**, 4220 (1996).
[18]S. J. Limb, K. K. Gleason, D. J. Edell, and E. F. Gleason, J. Vac. Sci. Technol. A **15**, 1814 (1997).
[19]N. B. Colthup, L. H. Daly, and S. E. Wiberly, *Introduction to Infrared and Raman Spectroscopy*, 3rd ed. (Academic, New York, 1990).
[20]*Lange's Handbook of Chemistry*, 14th ed. (McGraw–Hill, New York, 1992).
[21]W. K. Fisher and J. C. Corelli, J. Polym. Sci., Part A: Polym. Chem. **19**, 2465 (1993).
[22]R. d'Agostino, F. Cramarossa, F. Fracassi, and F. Illuzzi, *Plasma Deposition, Treatment and Etching of Polymers* (Academic, San Diego, 1990), pp. 96–162.
[23]R. d'Agostino, L. Martinu, and V. Pische, Plasma Chem. Plasma Process. **11**, 1 (1991).
[24]N. Amyot, J. E. K. Sapieha, M. R. Wertheimer, Y. Ségui, and M. Moisan, IEEE Trans. Dielectr. Electr. Insul. **27**, 1101 (1992).
[25]G. Turban, B. Grolleau, P. Launay, and P. Briaud, Phys. Rev. **20**, 609 (1985).
[26]M. Schaepkens, T. E. F. M. Standaert, N. R. Rueger, and P. G. M. Sebel, J. Vac. Sci. Technol. A **17**, 26 (1999).
[27]B. Beagley, M. O. Jones, and P. Yavari, J. Mol. Struct. **71**, 203 (1981).
[28]I. C. Plumb and K. R. Ryan, Plasma Chem. Plasma Process. **6**, 11 (1986).